Journal of Solid State Chemistry **156,** 230–236 (2001)
doi:10.1006/jssc.2000.8993, available online at http://www.idealibrary.com on IDEAL®

Synthesis and Characterization of $SrBi_2Se_4$

Ying C. Wang, Roald Hoffmann, and Francis J. DiSalvo[1]

Department of Chemistry and Chemical Biology, Baker Laboratory, Cornell University, Ithaca, New York 14853

Received May 8, 2000; in revised form September 1, 2000; accepted October 6, 2000; published online December 21, 2000

$SrBi_2Se_4$ was synthesized at 945°C and its structure was determined using single-crystal X-ray diffraction data obtained at 165 K. $SrBi_2Se_4$ is isotypic to 12-$BaBi_2S_4$ and $Eu_{1.1}Bi_2S_4$. The compound crystallizes in $P6_3/m$ ($Z = 12$) with $a = 25.970(2)$ Å and $c = 4.2437(3)$ Å. Final $R_1 = 0.0630$ and $wR_2 = 0.1246$ ($I > 2\sigma(I)$). The coordination environments of Bi are distorted Se octahedra. These octahedra build up a uniaxial three-dimensional network with tunnels along the z direction, which are filled by Sr^{2+}. There is also a second tunnel along the z direction which is partially occupied by Bi atoms. The coordination spheres of Sr are bicapped trigonal prisms of Se. Transport measurements indicate that $SrBi_2Se_4$ is semiconducting. This work adds one high-symmetry compound to the family of complex chalcogenides, in which low-symmetry compounds are common. © 2001 Academic Press

Key Words: **chalcogenide; transport property; thermoelectric materials; crystal structure; multivalley band structure.**

1. INTRODUCTION

In part due to environmental concerns, thermoelectric cooling and power generation have received special attention (1). Thermoelectric devices use no freons (CFCs or HCFCs) and are mechanically more reliable than conventional cooling. Currently, the use of thermoelectric devices is limited by their low efficiencies, which is in turn determined by properties of the semiconductors used in these devices. One direction in the search for good thermoelectric materials with high figures of merit $ZT = S^2T/\rho\kappa$ (S is Seebeck coefficient, T is temperature, ρ is electrical resistivity, and κ is thermal conductivity) has been to focus on complex chalcogenides based on Sb_2Q_3 and Bi_2Q_3 (Q = Se and Te) (2). Some of these compounds display high thermopower, high electrical conductivity, and low thermal conductivity, but unfortunately none of them has achieved higher ZT than the Bi_2Te_3-based alloys, the best known thermoelectric materials at room temperature so far. A possible reason is that the majority of ternary and quaternary Bi- or Sb-containing chalcogenides crystallize in low-symmetry space groups, monoclinic or orthorhombic systems (2, 3).

A perusal of the thermoelectric materials used in current devices demonstrates that all the good thermoelectric materials have high crystal symmetry. For example, Bi_2Te_3 in $R\bar{3}m$, PbTe in $Fm\bar{3}m$, Si–Ge in $Fd\bar{3}m$, and Sb–Bi in $R\bar{3}m$. High crystal symmetry may lead to multivalley features in the band structure, which can boost the figure of merit significantly (1a, 4, 5). The number of equivalent valleys is defined as N_v, the degeneracy of band extrema near the Fermi level. Band extrema are associated with zero-slope points (stationary values) in the electronic energy bands $E_j(\boldsymbol{k})$ of a crystal, where j is the band number and $\boldsymbol{k}$ is the reciprocal lattice vector. Stationary values may be required by crystal symmetry (such points are called "essential"), or they may be accidental, due to the specific potential distribution in the crystal (6). The occurrence and maximum number of essential stationary value points are determined by the Patterson symmetry associated with the crystal symmetry. The maximum number of accidental stationary value points are limited by the crystal Laue group, 48 for $m3m$, 24 for $m3$ and $6/mmm$, 16 for $4/mmm$, 12 for $6/m$ and $-3m$, 8 for mmm, 4 for $2/m$, and 2 for -1. Such band extrema, if they exist, must be at a general $\boldsymbol{k}$ point of no symmetry. Intrinsically and statistically, compounds of high crystal symmetry have a greater possibility of resulting in higher N_v. Unfortunately, at the present we can not predict what crystal potential will produce high N_v of equivalent band extrema.

This work reports the synthesis of $SrBi_2Se_4$, a high crystal symmetry ($P6_3/m$) chalcogenide. Its structural and thermoelectric properties are investigated.

2. EXPERIMENTAL

Reagents. All the chemicals in this work were used as obtained: strontium distilled dendritic pieces, 99.99% purity, ampouled under argon, Aldrich, Milwaukee, WI; selenium pellets, 99.9999% purity, Atomergic Chemicals Corp., Plainview, NY; bismuth powder, 99.999% purity, -8 mesh, Alfa Products, Danvers, MA.

[1] To whom correspondence should be addressed. Fax: 607-255-4137. E-mail: fjd3@cornell.edu.

0022-4596/01 $35.00
Copyright © 2001 by Academic Press
All rights of reproduction in any form reserved.

Synthesis. Due to the air sensitivity of strontium, all work was carried out under an argon atmosphere in a vacuum dry box. $SrBi_2Se_4$ was synthesized from a mixture of 0.1067 g Sr, 0.5088 g Bi, and 0.3845 g Se with the stoichiometry Sr:Bi:Se::1:2:4. The elemental mixture was put in a vitreous carbon crucible and was sealed in an evacuated quartz tube. Then it was gradually heated to 945°C over 24 h, kept at that temperature for 36 h, slowly cooled to 820°C at 1.3°C/h, and cooled to 620°C at 2°C/h. Powder X-ray diffraction patterns (Scintag XDS 2000 with Cu$K\alpha$ radiation) of the black shiny product could not be indexed to any known phases. A needle-like crystal was obtained from the product mixture and was used for a single-crystal diffraction study, which yielded the formula $SrBi_2Se_4$. The simulated powder X-ray diffraction pattern (7) according to the single-crystal structure solution matched the powder X-ray pattern of the experimental product.

Property measurements. Measurements were conducted on a sintered pellet of polycrystalline $SrBi_2Se_4$. The sample was synthesized at 945°C, slowly cooled to 545°C at 2°C/h, ground and pressed into a pellet in an argon atmosphere at room temperature, and sintered at 600°C for 2 days. The pellet was cut into a rectangular parallelepiped (2.70 mm × 5.50 mm × 5.95 mm). Phase purity was checked by powder X-ray diffraction (Scintag XDS 2000 with Cu$K\alpha$ radiation).

The electrical resistivity was measured on a home-built apparatus using a four-probe ac technique (8). Current contacts were made by attaching 0.05-mm-thick copper foil strips at the ends of the sample with silver epoxy (H20E, Epoxy Technology). Voltage leads were made by placing 38 AWG copper wires coated with silver epoxy on the flat surfaces of the sample bar. Due to uncertainties in measuring the area factor and the voltage contact spacing, a $\pm$ 10% error in absolute values of resistivity is possible.

The thermopower was measured on the sample using the steady-state technique in a home-built setup (8). The sample was first mounted on a copper base with silver epoxy. A 5-kΩ resistor (heater) was attached to the opposite end of the sample with silver epoxy. Two 40 AWG Au, Fe(0.07%):Chromel-*p* thermocouples were attached to the epoxy joints at either end of the sample. The sample chamber was then evacuated to less than 4×10^{-5} Torr. Small and steady temperature gradients (maximum 2 K) were achieved by incrementally increasing the power to the resistor. The resulting temperatures on both ends of the sample were measured using the two attached thermocouples. The voltage across the sample was measured using the Chromel-*p* wires of the two thermocouples. From a plot of the voltage across the sample versus the temperature gradient, we could calculate the slope, which is equal to the thermopower of the sample plus the thermopower of the Chromel-*p* wire. The absolute thermopower of the Chromel-*p* wire was subtracted from the measured slope to give the absolute thermopower of the sample. The overall accuracy of the thermopower measurement has been estimated from standards to be within $\pm$ 5% (8).

Crystallographic study. Crystals from several batches were selected under a microscope and mounted on glass fibers by using poly(butenes) (viscosity at 99°C 109–125 cst, *d* 0.885, catalogue no. 38868-8, Aldrich) for data collection at low temperatures. X-ray diffraction data sets were collected on a Bruker SMART diffractometer equipped with a 1 K CCD detector and a 3 KW sealed tube X-ray generator (Mo$K\alpha$, 30 s exposure time, $\Delta\omega = 0.3°$). No intensity decay was observed during the data collection for any crystals. The unit cells were refined during the integration (program SAINT) based on all strong reflections in the Laue group 6/*m*. Both an analytical absorption correction (XPREP) and an empirical absorption correction by using SADABS were attempted (9); the two corrections resulted in essentially the same atomic positions. Since the empirical absorption correction (SADABS) yielded slightly lower R_{int} and R_1/wR_2, we report the structural solution based on the empirical absorption correction. After data integration, the R_{int} was 0.1509. After SADABS was applied to conduct an empirical absorption correction, the R_{int} dropped to 0.0681. The structure was solved and refined using SHELX-93 (9). The systematic extinctions are consistent with the hexagonal space group $P6_3/m$. To confirm the correct assignment of space group, we also attempted to solve the structure in $P\bar{3}$, but it yielded higher values of the reliability factors: $R_1 = 0.0715$ ($I > 2\sigma(I)$) and R_1, $wR_2 = 0.1317, 0.1629$ for all data. The PLATON software package (10) was run to check for possible higher lattice symmetry or missed additional symmetry. It suggested that the correct space group is $P6_3/m$.

Two Sr atoms, four Bi atoms, and eight Se atoms were located on 6*h* positions by direct methods. This corresponds to the stoichiometry $SrBi_2Se_4$. After a refinement including extinction and anisotropic displacement factors for all atoms, $R_1 = 0.0758$ ($I > 2\sigma(I)$), $R_1/wR_2 = 0.1184/0.1907$ for all data, and GooF = 1.362.

However, on the difference Fourier map, there is a large difference peak Q1 = 26.83 e$Å^{-3}$ at $(0, 0, \frac{1}{4})$, whose Wyckoff symmetry is 2*a*. The Q1 site is in a tunnel along the *z* direction formed by Se3 atoms. As shown in Fig. 1, Q1 is surrounded by three nearest neighboring atoms of Se3 at the distance of 3.02 Å in a planar triangular arrangement and six next nearest neighboring atoms of Se3 at the distance of 3.69 Å in a trigonal prism arrangement. The Q1–Q1 distance is 2.122 Å, which is too close for any atoms of the current system to fully occupy the position at Q1. EUTAX (11) calculation showed that the Madelung potentials were $-$ 27.437 V at Q1 and about $-$ 18 V at the two Sr positions, respectively. This suggests that no anion can be placed

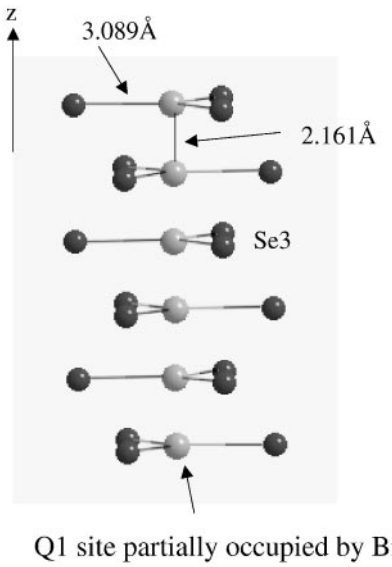

FIG. 1. The Se3 tunnel. The dark dots are Se3 and the gray dots in the middle are Q1.

at the position of Q1; Sr^{2+} is also unlikely to be at Q1. Assuming the canonical oxidation states Sr^{2+}, Bi^{3+}, and Se^{2-}, the charge balance condition would require the stoichiometry to be $SrBi_2Se_4$. A close examination of the atomic displacement parameters (ADP) of Sr and Bi atoms revealed that the two Sr atoms had similar ADP values, whereas the ADP values of Bi1 were more than twice as large as those of the other three Bi atoms. Bi1 is connected to Se3, and it is the Bi atom closest to Q1.

We propose a partially disordered model for the structure: the Bi1 site is partially occupied and the missing atom is provisionally situated at the Bi5 site $(0, 0, \frac{1}{4})$ to maintain the stoichiometry $SrBi_2Se_4$. Refining the occupancies of Bi5 and Bi1 resulted in 92.1(3)% Bi1 and 23.7(9)% Bi5, with significantly improved reliability factors $R_1 = 0.0630$ $(I > 2\sigma(I))$, $R_1, wR_2 = 0.1050, 0.1576$ for all data, and GooF = 1.122. The largest difference peak and hole were $2.732/-2.541\ e\text{Å}^{-3}$. On the other hand, a refinement without the stoichiometry constraint resulted in the same occupancies, 92.1(5)% Bi1 and 23.7(9)% Bi5. It is worth mentioning that extra electron density in the tunnel (Q1 position) has also been found in two isostructural compounds $BaBi_2S_4$ (12) and $Eu_{1.1}Bi_2S_4$ (13).

We also considered other disorder and nonstoichiometry models. First, Sr5, rather than Bi5, was put at Q1 in the tunnel. Based on reliability factors and GooF alone, this model is also plausible. However, the ADF of Bi1 remains large and the site potential at Q1 would suggest that a trivalent cation is preferred at this site. With the stoichiometry constraint of $SrBi_2Se_4$, the refinement resulted in 91.5(4)% Sr1, 94.1(6)% Sr2, 43(2)% Sr5 with $R_1 = 0.0640$ $(I > 2\sigma(I))$, $R_1/wR_2 = 0.1055/0.1595$ for all data, and GooF = 1.136. Without the stoichiometry constraint of $SrBi_2Se_4$, the refinement resulted in 93%(1) Sr1, 130(1)% Sr2, and 69(2)% Sr5, with reliability factors $R_1 = 0.0688$ $(I > 2\sigma(I))$ and $R_1, wR_2 = 0.1103, 0.1730$ for all data, and GooF = 1.232. Again, the reliability factors and GooF from the refinement of the unconstrained Sr disorder and nonstoichiometry model are only a little higher than those from the refinement of a stoichiometry model with Bi or Sr disorder alone. However, the site occupancies at Sr2 and Sr5 are unreasonably high, because the site occupancy at Sr2 cannot exceed 1 and the site occupancy at Sr5 should not exceed 0.5 due to the close Sr5–Sr5 distance of 2.122 Å.

Based on the above considerations, we prefer the stoichiometric model of $SrBi_2Se_4$ with the Bi disorder at Bi1 and Bi5, which converges with the best statistical factors and the smoothest Fourier difference map. Furthermore, site potentials suggest that a trivalent cation is best suited to the Q1 site. In this model, charge balance is maintained: 6.9% of the Bi atoms at the Bi1 site migrate to a Bi5 site in the tunnel formed by Se3.

Data collection parameters and details of the structure solution and refinement for all compounds are listed in Table 1. The crystal data were standardized by the program STRUCTURE TIDY (14). Atomic coordinates

TABLE 1
Crystal Data and Structure Refinement for $SrBi_2Se_4$

Empirical formula	$SrBi_2Se_4$
Formula weight	821.42
Temperature	165(2) K
Wavelength	0.71073 Å
Crystal system	Hexagonal
Space group	$P6_3/m$
Unit cell dimensions	$a = 25.970(2)$ Å $\alpha = 90.000(1)^\circ$ $b = 25.970(2)$ Å $\beta = 90.000(2)^\circ$ $c = 4.2437(3)$ Å $\gamma = 120.000(1)^\circ$
Volume	2478.7(3) $Å^3$
Z	12
Density (calculated)	6.603 Mg/m^3
Absorption coefficient	66.441 mm^{-1}
$F(000)$	4080
Crystal size	$0.200 \times 0.015 \times 0.015\ mm^3$
Theta range for data collection	0.91 to 26.27°
Index ranges	$-26 \le h \le 31$, $-32 \le k \le 13$, $-5 \le l \le 3$
Reflections collected	8482
Independent reflections	1821 [$R_{int} = 0.1266$]
Refinement method	Full-matrix least-squares on F^2
Data/restraints/parameters	1821/1/90
Goodness-of-fit on F^2	1.122
Final R indices [$I > 2\sigma(I)$]	$R_1 = 0.0630$, $wR_2 = 0.1246$
R indices (all data)	$R_1 = 0.1050$, $wR_2 = 0.1576$
Extinction coefficient	0.00027(6)
Largest diff. peak and hole	2.731 and $-2.541\ e\text{Å}^{-3}$
Weighting scheme	$w^{-1} = [\sigma^2(F_o^2) + (0.0700P)^2 + 0.000P]$, where $P = [\max(F_o^2, 0) + 2F_c^2]/3$

TABLE 2
Atomic Coordinates and Equivalent Isotropic Displacement Parameters ($Å^2 \times 10^3$) for $SrBi_2Se_4$ at 165 K

	x	y	z	U(eq)	Occupancy
Sr1	0.3557(2)	0.1205(2)	$\frac{1}{4}$	14(1)	1
Sr2	0.5572(2)	0.2332(2)	$\frac{1}{4}$	14(1)	1
Bi1	0.0216(1)	0.1798(1)	$\frac{1}{4}$	19(1)	0.921(3)
Bi2	0.0504(1)	0.5887(1)	$\frac{1}{4}$	15(1)	1
Bi3	0.1469(1)	0.4946(1)	$\frac{1}{4}$	15(1)	1
Bi4	0.3327(1)	0.2731(1)	$\frac{1}{4}$	15(1)	1
Bi5	0	0	$\frac{1}{4}$	61(7)	0.237(9)
Se1	0.0013(2)	0.3682(2)	$\frac{1}{4}$	15(1)	1
Se2	0.1204(2)	0.3064(2)	$\frac{1}{4}$	16(1)	1
Se3	0.1341(3)	0.0751(2)	$\frac{1}{4}$	35(1)	1
Se4	0.2201(2)	0.2575(2)	$\frac{1}{4}$	15(1)	1
Se5	0.2518(2)	0.5955(2)	$\frac{1}{4}$	13(1)	1
Se6	0.3043(2)	0.4571(2)	$\frac{1}{4}$	14(1)	1
Se7	0.4501(2)	0.2651(2)	$\frac{1}{4}$	14(1)	1
Se8	0.5498(2)	0.0919(2)	$\frac{1}{4}$	16(1)	1

Note. Here, U(eq) is defined as one-third of the trace of the orthogonalized U_{ij} tensor.

and equivalent isotropic displacement parameters U(eq) are listed in Table 2. Selected bonding distances are tabulated in Table 3.

3. RESULTS AND DISCUSSION

Structure description. $SrBi_2Se_4$ is isostructural to 12-$BaBi_2S_4$ with $Z = 12$ and $Eu_{1.1}Bi_2S_4$ (12, 13). $SrBi_2S_4$, with hexagonal cell parameters $a = 24.925$ Å and $c = 4.095$ Å, was reported to exist (12). It possibly crystallizes in the same structure type, based on an analysis of the powder photographs, but its full crystal structure has not been studied. We have also found the isostructural phase $BaBi_2Se_4$ with $a = 26.230$ Å and $c = 4.326$ Å (15). The projection of the $SrBi_2Se_4$ structure on the xy plane is shown in Fig. 2. All the Bi atoms are surrounded by six Se atoms to form distorted $BiSe_6$ octahedra (Table 3). These octahedra build up a uniaxial three-dimensional network by edge-sharing or corner-sharing. Some of the space left by this arrangement of Bi and Se atoms is filled in by Sr atoms. The closest Sr–Sr distance is 4.244 Å, which is the unit cell dimension in the z direction. The two Sr atoms are coordinated to eight Se atoms. The positions of these eight Se atoms can be described as trigonal prisms with two rectangular faces capped by an Se atom.

TABLE 3
Selected Bond Lengths (Å) for $SrBi_2Se_4$

Sr1–Se6 × 2	3.151(4)	Bi1–Se3 × 2	2.831(3)
Sr1–Se4 × 2	3.186(4)	Bi1–Se3	2.875(5)
Sr1–Se2 × 2	3.349(4)	Bi1–Se2	2.992(4)
Sr1–Se7	3.302(5)	Bi1–Se4 × 2	3.091(3)
Sr1–Se1	3.319(5)	Bi2–Se6	2.720(4)
Sr2–Se5 × 2	3.179(4)	Bi2–Se8 × 2	2.903(3)
Sr2–Se6 × 2	3.193(4)	Bi2–Se1 × 2	3.011(3)
Sr2–Se5 × 2	3.299(4)	Bi2–Se8	3.557(4)
Sr2–Se7	3.278(5)	Bi3–Se5	2.673(4)
Sr2–Se8	3.575(5)	Bi3–Se7 × 2	2.821(3)
		Bi3–Se8 × 2	3.135(3)
Bi5–Bi5	2.1218(2)	Bi3–Se1	3.557(4)
Bi5–Se3	3.024(6)	Bi4–Se4	2.745(4)
		Bi4–Se2 × 2	2.922(3)
		Bi4–Se1 × 2	3.006(3)
		Bi4–Se7	3.158(4)

A striking feature in the structure is the Se3 tunnel centered around the sixfold axis along the z direction. The Se3 tunnel can be described as consisting of highly distorted octahedra condensed into a column through face-sharing (Fig. 1, Fig. 3). Suppose that the octahedral center is C, then the six Se–C distances are 3.193 Å and the Se–C–Se angles are 70.35° or 109.65° (Fig. 3). Obviously, the angles deviate severely from 90° and 180°, the angles for ideal octahedra. The tunnel is partially occupied by Bi atoms (Bi5), which are located on the triangular octahedral faces rather than the octahedral center. We attempted to put Bi at the octahedral center, (0, 0, 1/2), but the SHELX refinement yielded larger reliability factors R_1, $wR_2 = 0.0667$, 0.1331 ($I > 2\sigma(I)$), and a large difference peak 15.34 e/Å^3 at (0, 0, $\frac{1}{4}$) remained on the center of octahedral faces. This clearly indicates that Bi5 prefers to be on the triangular faces rather than at the centers of the distorted selenium octahedra.

In order to further investigate the large values of U(eq) of Bi5 in the tunnel (the anisotropic thermal parameters in Å $\times 10^3$ for Bi5 are $U_{11} = 43(7)$, $U_{22} = 43(7)$, $U_{33} = 96(17)$, $U_{23} = 0$, $U_{13} = 0$, and $U_{12} = 21(3)$), we collected data on the same crystal at 95, 165 and 255 K. The atomic coordinates remained the same within 3σ. No structure change or phase transition was observed. The equivalent isotropic displacement parameters U(eq) (Å^2) for Bi5 did not display an obvious temperature dependence, 0.058(7) at 95 K, 0.061(7) at 165 K, and 0.059(8) at 255 K. The U(eq) (Å^2) for Se3 (directly surrounding Bi5) showed a decrease of 25.6% from 255 to 95 K: 0.043 at 225 K, 0.035 at 165 K, and 0.032 at 95 K. The smaller U(eq) values for all the other atoms showed an obvious decrease of approximately 31–42% as the temperature decreased from 255 to 95 K. We conclude that the large temperature-independent U(eq) of Bi5 in the Se3 tunnel is due to Bi5 static disorder.

All the $BiSe_6$ octahedra in the compound are distorted to a different extent depending on the crystallographic sites. Distortion of octahedra is common in Bi containing chalcogenides, as a result of the $6s^2$ lone pair effect (2). The typical pattern of distortion is sketched in Fig. 4. Among the six Bi–Q bonds (Q = S, Se, Te), there are four different bonding distances, $d1$, $d2$, $d3$, and $d4$. Two equivalent bonds have $d2$ and two equivalent bonds have $d3$; $d1$ and $d4$ correspond

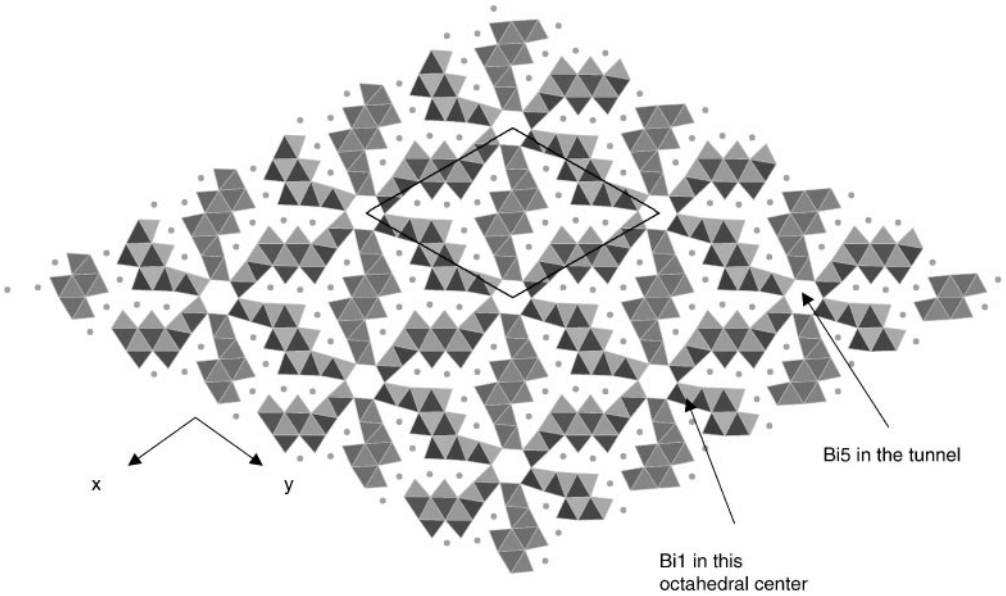

FIG. 2. Projection of $SrBi_2Se_4$ (12-phase) on the xy plane. The discrete dots are Sr atoms.

to the other two bonds that are *trans* to each other. Here we assume $d1 < d4$. The lone pair on the central atom Bi, when stereochemically active, presumably bulges out toward the $d4$ side. The difference of bonding distances, $d4$–$d1$, can range from almost zero to over 1 Å, as demonstrated in numerous chalcogenides.

Polyhedral distortion can be evaluated in terms of angles or bonding distances. Considering the geometrical characteristics of the distorted BiQ_6 octahedra as described above, we use the $d4$–$d1$ difference to measure the distortion of the four BiQ_6 octahedra in $SrBi_2Se_4$ and the other two isostructural compounds 12-$BaBi_2S_4$ (12) and $Eu_{1.1}Bi_2S_4$ (13). The $d4$–$d1$ values for the four octahedra in each compound are listed in Table 4. The magnitudes of distortion vary significantly from site to site in each compound, from 0.166 to 1.098 Å. However, all three compounds display a similar pattern, large $d4$–$d1$ (above 0.84 Å) on Bi2 and Bi3, small $d4$–$d1$ (below 0.45 Å) on Bi1 and Bi4.

$BaBi_2S_4$ crystallizes in two polymorphs (12), 9-$BaBi_2S_4$ and 12-$BaBi_2S_4$, where 9 and 12 represent Z (number of formula units/cell) for each compound, respectively. Both compounds crystallize in $P6_3/m$. For comparison, a drawing of the 9-$BaBi_2S_4$ structure is shown in Fig. 5. The 9-phase and 12-phase have similar structural motifs: BiS_6 octahedra connect with each other to build up to a three-dimensional uniaxial anionic network and electropositive elements fill in the space left. A partially occupied tunnel also appears in the 9-phase. The 9-phase is denser than the 12-phase: the calculated density is 6.02 Mgm^{-3} for the 9-phase and 5.89 Mgm^{-3} for the 12-phase (12). In the Sr–Bi–Se system, we have only been able to synthesize 12-$SrBi_2Se_4$. Similarly, 12-$SrBi_2S_4$ has been reported (12), but 9-$SrBi_2S_4$ was suggested not to exist. For $Eu_{1.1}Bi_2S_4$, only the compound isotypic to 12-$BaBi_2S_4$ has been reported (13). It seems that the 12-phase is more prevalent than the 9-phase.

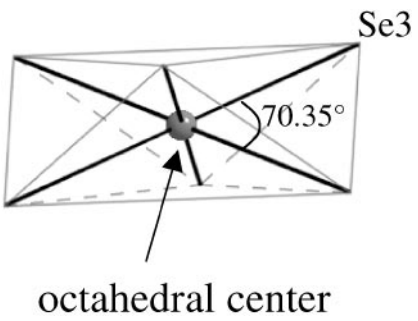

FIG. 3. The highly distorted octahedra in the Se3 tunnel.

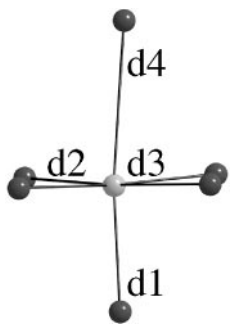

FIG. 4. The distortion of BiQ_6 octahedra; $d1$, $d2$, $d3$, and $d4$ are the four nonequivalent bonding distances.

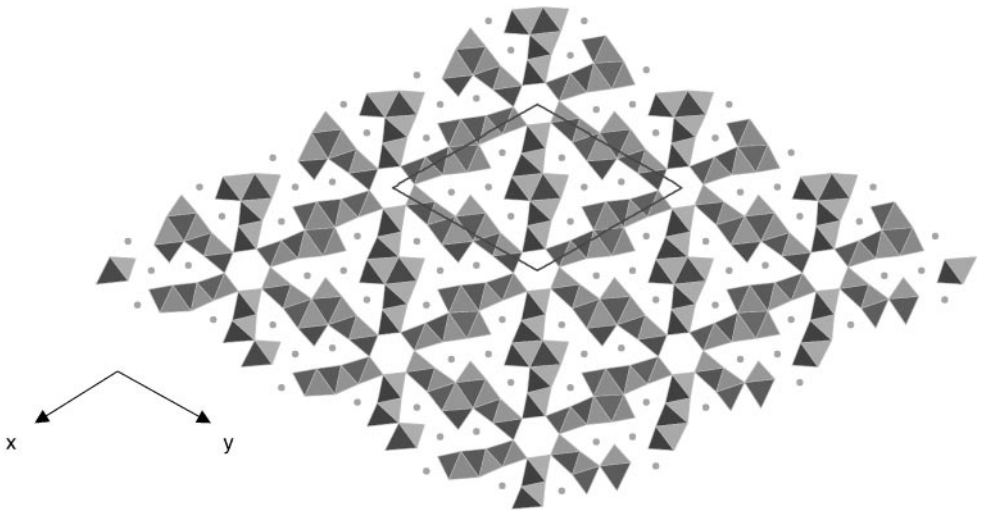

FIG. 5. Projection of 9-$BaBi_2S_4$ (9-phase) on the xy plane. The discrete dots are Ba atoms.

We compared $SrBi_2Se_4$ with other compounds of the same stoichiometry in similar systems containing alkaline earth metal, pnicogen, and chalcogen (including oxygen). $SrBi_2O_4$ (16) is a layered compound crystallizing in $C2/m$. $SrAs_2S_4$ (17) crystallizes in the sphalerite (zinc blende) type with a Sr and As mixed occupancy of 0.75 at (0, 0, 0). $BaSb_2S_4$ and $BaSb_2Se_4$ (18) are layered compounds crystallizing in $P2_1/c$. Thus there is little similarity between $SrBi_2Se_4$ and $SrBi_2O_4$, $BaSb_2Se_4$, or $BaSb_2S_4$.

Although ternary and quaternary pnicogen chalcogenides of high crystal symmetry do not occur very often, there is another high crystal symmetry structure type, the two isotypic hexagonal chalcogenide phases β-$CsPbBi_3Se_6$ and $CsPbBi_3S_6$ (2a). These two compounds crystallize in $P6_3/mmc$, but they are layered compounds with $(PbBi_3Se_6)^-$ or $(PbBi_3S_6)^-$ slabs separated by Cs^+ layers. So they are very different from $SrBi_2Se_4$, which has a uniaxial three-dimensional network of $(Bi_2Se_4)^{2-}$, leaving tunnels along the z direction for Sr^{2+} to fill in.

Transport property measurements. The temperature dependence of electrical resistivity (ρ) for a pressed pellet of $SrBi_2Se_4$ is shown in Fig. 6. The electrical resistivity increases from 0.041 $\Omega\cdot$cm at room temperature to 0.068 $\Omega\cdot$cm at 8.5 K. The electrical resistivity is more than an order of magnitude higher than that of single-crystal Bi_2Se_3 ($1.6\text{–}2.0\times10^{-3}$ $\Omega\cdot$cm) (19). The weak temperature dependence of our sample suggests the behavior of a nearly degenerate semiconductor. The thermopower of $SrBi_2Se_4$ was measured to be -62.1 μV/K at 299 K. The negative sign reveals that electrons are the dominant carriers in the sample. The magnitude of the thermopower is characteristic of a highly doped semiconductor, which is in agreement with the electrical resistivity measurement.

Even with low thermal conductivity, the ZT of this sample is estimated to be well below 1. However, ZT is a function of the doping level and we have not yet attempted to control or change this level. Disorder may present challenges to doping, by allowing compensating defects. If that were the case in any material, the possibility of attaining

TABLE 4
The $d4$–$d1$ Values (Å) for the BiQ_6 Octahedra in Three Compounds

	$BaBi_2S_4$	$Eu_{1.1}Bi_2S_4$	$SrBi_2Se_4$
Bi1	0.166	0.221	0.117
Bi2	0.996	1.096	0.837
Bi3	1.098	1.000	0.884
Bi4	0.259	0.444	0.413

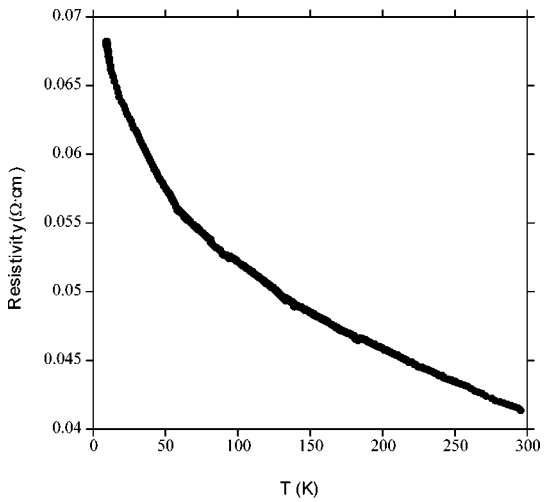

FIG. 6. Electrical resistivity versus T for the sintered pellet of $SrBi_2Se_4$.

high ZT would be significantly reduced. In particular, the potential benefits of high symmetry could not be realized in the present case. However, it is interesting that a new high-symmetry compound has been added to the family of complex bismuth chalcogenides, in which low-symmetry compounds are very common.

ACKNOWLEDGMENTS

This work was funded by the Office of Naval Research. This work made use of the Cornell Center for Materials Research Shared Experimental Facilities, supported through the National Science Foundation Materials Research Science & Engineering Centers Program (DMR-9632275).

REFERENCES

1. (a) F. J. DiSalvo, *Science* **285,** 703 (1999); (b) *in* "MRS 1998 Fall Meeting, Boston, MA: Thermoelectric Materials," p. 477f, 1998; (c) G. Mahan, B. Sales, and J. Sharp, *Phys. Today* **50,** 42 (1997); (d) C. Wood, *Rep. Prog. Phys.* **51,** 459 (1988); (e) H. J. Goldsmid, "Electric Refrigeration." Pion, London, 1986.
2. (a) D.-Y. Chung, L. Iordanidis, K. K. Rangan, P. W. Brazis, C. R. Kannewurf, and M. G. Kanatzidis, *Chem. Mater.* **11,** 1352 (1999); (b) D.-Y. Chung, K.-S. Choi, L. Iordanidis, J. L. Schindler, P. W. Brazis, C. R. Kannewurf, B. Chen, S. Hu, C. Uher, and M. G. Kanatzidis, *Chem. Mater.* **9,** 3060 (1997); (c) D.-Y. Chung, L. Iordanidis, K. Choi, and M. G. Kanatzidis, *Bull. Korean Chem. Soc.* **19,** 1283 (1998); (d) D.-Y. Chung, S. Jobic, T. Hogan, C. R. Kannewurf, R. Brec, J. Rouxel, and M. G. Kanatzidis, *J. Am. Chem. Soc.* **119,** 2505 (1997); (e) T. J. MaCathy, T. A. Tanzer, and M. G. Kanatzidis, *J. Am. Chem. Soc.* **117,** 1294 (1995); (f) J. H. Chen and P. K. Dorhout, *J. Alloys Comp.* **249,** 199 (1997).
3. ICSD/RETRIEVE 2.01, Gmelin Institute/Fiz Karlsruhe, Release Feb. 1998.
4. G. D. Mahan, *Solid State Phys.* **51,** 82 (1998).
5. D. M. Rowe and C. M. Bhandari, "Modern Thermoelectrics," p. 43. Reston Publishing Co., VA, 1983.
6. A. P. Cracknell, *J. Phys. C Solid State Phys.* **6,** 826 (1973).
7. D. C. Palmer, Crystal Diffract 2.0.0, 1995.
8. C. D. W. Jones, K. A. Regan, and F. J. DiSalvo, *Phys. Rev. B* **58,** 16057 (1998).
9. (a) G. M. Sheldrick, SHELX-93, Institut für Anorganische Chemie der Universität Göttingen, 1993; (b) G. M. Sheldrick, the computer program SADABS used by Siemens CCD diffractometers, Institut für Anorganische Chemie der Universität Göttingen.
10. A. L. Spek, *Acta Crystallogr. A* **46** (Suppl.), C34 (1990).
11. (a) M. O'Keeffe and N. Brese, EUTAX 1.2 program, 1992; (b) N. E. Brese and M. O'Keeffe, *Acta Crystallogr. B* **47,** 192 (1991); (c) M. O'Keeffe and N. E. Brese, *Acta Crystallogr. B* **48,** 152 (1992); (d) M. O'Keeffe and N. E. Brese, *J. Am. Chem. Soc.* **113,** 3226 (1991).
12. B. Aurivillius, *Acta Chem. Scand. A* **37,** 399 (1983).
13. P. P. Lemoine, D. Carré, and M. Guittard, *Acta Crystallogr. C* **42,** 259 (1986).
14. E. Parthé, STRUCTURE TIDY program, PC version, University of Geneva, 1992.
15. Y. Wang, Ph.D. dissertation, Cornell University, 2000.
16. T. A. M. Haemers and D. J. W. IJdo, *Mater. Res. Bull.* **26,** 989 (1991).
17. L. D. C. Bok and J. H. de Wit, *Z. Anorg. Allg. Chem.* **324,** 162 (1963).
18. (a) G. Cordier, C. Schwidetzky, and H. Schaefer, *J. Solid State Chem.* **54,** 84 (1984); (b) G. Cordier and H. Schäfer, *Z. Naturforsch. B* **34,** 1053 (1979).
19. J. Black, E. M. Conwell, L. Seigle, and C. W. Spencer, *J. Phys. Chem. Solids* **2,** 240 (1957).